Assessment of the 1783 Scilla landslide-tsunami effects on Calabria and Sicily coasts through numerical modeling

Filippo Zaniboni[1,2], Gianluca Pagnoni[1], Glauco Gallotti[1], Maria Ausilia Paparo[1], Alberto Armigliato[1], Stefano Tinti[1]

[1]Dipartimento di Fisica e Astronomia, Università di Bologna, Bologna, Viale Berti-Pichat 6/2, 40127 Bologna, Italy
[2]Istituto Nazionale di Geofisica e Vulcanologia – Sezione di Bologna, Bologna, via Donato Creti 12, 40128 Bologna, Italy

*Correspondence to*: Filippo Zaniboni (filippo.zaniboni@unibo.it)

Abstract.

The 1783 Scilla landslide-tsunami (Calabria, South Italy) is a well-studied event, that caused more than 1500 fatalities in the beaches close to the town. This paper complements a previous work that was based on numerical simulations and was focused on the very local effects of the tsunami in Scilla. In this study we extend the computational domain to cover a wider portion of western Calabria and north-eastern Sicily, including the western side of the Messina Straits. This investigation focuses on the Capo Peloro area (the easternmost cape of Sicily), where the highest tsunami effects outside Scilla were reported. Important tsunami observations such as the wave height reaching 6 m at Torre degli Inglesi, and the inland flooding of over 600 m, have been successfully modelled, but only by means of a high-resolution (10 m) topo-bathymetric grid, since coarser grids resulted inadequate for the purpose. Interestingly, the inundation of the small lake of Pantano Piccolo could not be reproduced by using the today coastal morphology, since a coastal dune acts nowadays as a barrier for the tsunami. Historical analysis suggests that this dune was not in place at the time of the tsunami occurrence and that a ground depression extending from the lake to the northern coast is the remnant of an ancient channel that was used as a pathway in Roman times. The removal of such obstacle and the remodeling of the coeval morphology allows the simulations to reproduce the tsunami penetration up to the lake, therefore supporting the hypothesis that the 1783 tsunami entered the lake following the Roman channel track. A further result of this study is that the computed regional tsunami propagation pattern provides a useful hint for assessing tsunami hazard in the Messina Straits area, which is one of the most exposed to tsunami threat in Italy and in the Mediterranean Sea.

1 Introduction

The recent catastrophic tsunamis of Sumatra (2004), Japan (2011) and Sulawesi (2018) have raised the interest in such natural phenomena worldwide, including Europe. In the Mediterranean Sea, they are known to be of smaller magnitude than in the Pacific and in the Indian Oceans, but their effects can be as lethal, owing to the high coastal exposure and vulnerability, constantly growing in the last decades as the result of an increased coastal occupation (see Papadopoulos et al.,

2014). This poses the need for more detailed assessments of tsunami hazard and of the consequences of tsunami impact, which also implies the need for more accurate numerical simulation tools.

In this framework, the reconstruction of historical events that affected significantly the coasts of the Mediterranean Sea is very important since they can be used to test numerical simulation codes as well as for better estimates of the hazard and

5 risk. One of the most relevant cases in the Mediterranean, owing to the disastrous impact and the unusual availability of plenty of very detailed observations, is the 6 February 1783 landslide-induced tsunami in Scilla. This tragic event, causing the death of more than 1500 people, was the subject of several coeval reports, providing details on the devastating effects along the littoral but also on the coastal landslide that was the cause of the tsunami (see Graziani et al., 2006; Tinti et al., 2007; Gerardi et al., 2008). In a previous paper (Zaniboni et al., 2016) we investigated the tsunami impact close to the source

10 area, that is in the beaches of the town of Scilla, Marina Grande and Chianalea, where most of the tsunami fatalities were counted, see Figure 1. This was accomplished through numerical simulations under the assumption that the causative landslide was purely subaerial.
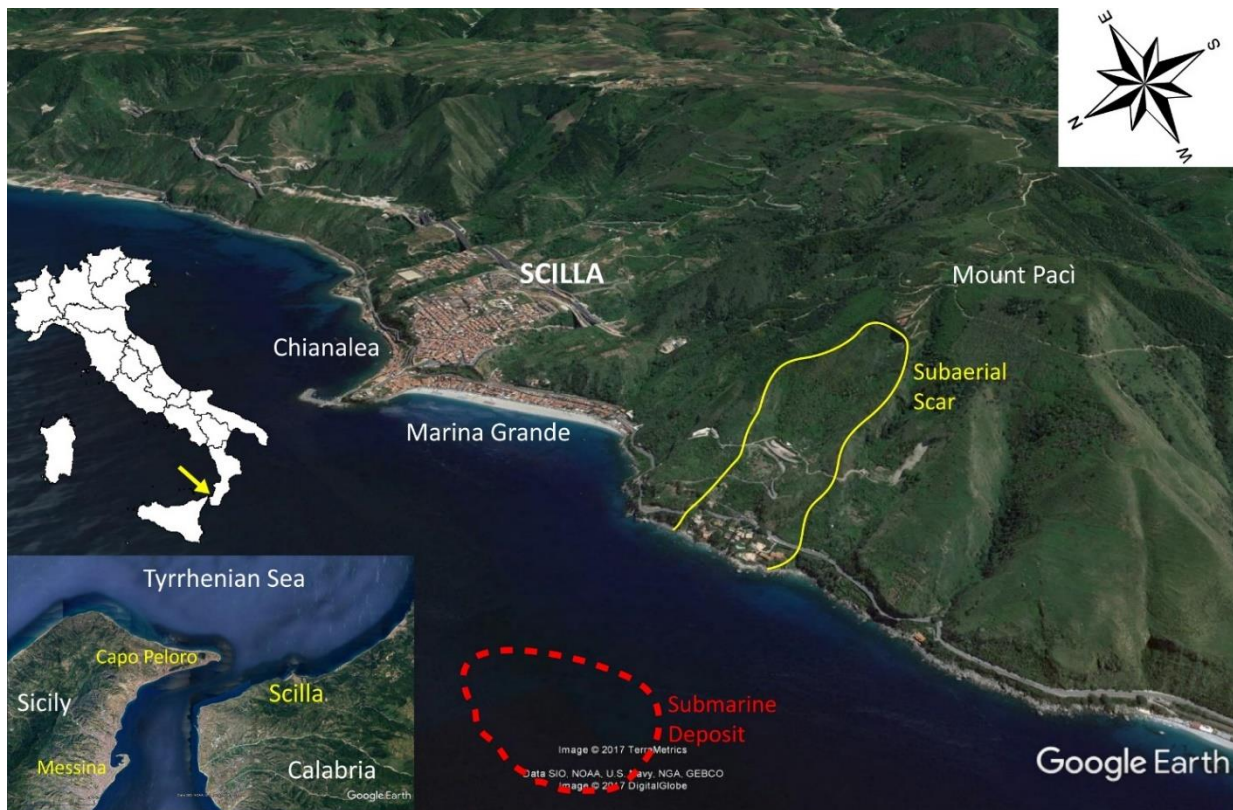
Figure 1. View of Scilla and its surroundings including the two main beaches of Marina Grande and Chianalea (see the position in
15 **the map of Italy on the left and in the zoom of the bottom left corner). The yellow contour delimits the landslide scar, measuring approximately 750 m x 400 m, about 1 km west of the town. The red contour marks the submarine deposit observed in the geo-marine surveys (Bozzano et al., 2011; Casalbore et al., 2014). Satellite views obtained by GoogleEarth©.**

As reported by eyewitnesses (descriptions and references are summarized in Table 1), tsunami waves affected at least as much as 40 km of the Calabrian coast, the cape of Sicily facing Scilla, named Capo Peloro, and the north-east coast of Sicily, just south of Messina. In this paper, we carry out three tsunami simulations, one to cover coasts located farther away from the source, and two to study the inundation in the area of Capo Peloro on the opposite side of the Messina Straits. To this purpose, we have performed a preliminary reconstruction of the coeval coastal morphology and topography of Capo Peloro by using features and observations recovered from historical sources. Comparison between numerical results and observations will allow us to evaluate the quality of the simulations.

2. The 6 February 1783 landslide-tsunami

In the first months of 1783 a catastrophic seismic sequence, with at least 5 main events, hit the Calabria region (South Italy), provoking about 30,000 casualties and the destruction of over 200 villages (Guidoboni et al., 2007). Cascade effects were also reported, including tsunamis and diffuse landslide occurrences in the Apennines, that form the backbone of the region (Tinti and Piatanesi, 1996; Graziani et al., 2006; Porfido et al., 2011).

The most tragic event took place during the night of February 6th, in the town of Scilla, on the Tyrrhenian coast of Calabria (see map in Figure 1). The day before, one of the strongest earthquakes of the sequence caused severe destruction in the village, forcing most of the population to find refuge in the wide beach of Marina Grande, west of the town. A strong aftershock in the night caused the collapse of the coastal flank of Mt Pacì in the sea, 1 km west of the Marina Grande beach. The ensuing tsunami killed more than 1500 people (Mercalli, 1906) and destroyed houses and churches (Tinti and Guidoboni, 1988; Graziani et al., 2006).

The huge death toll and the impression raised by the disaster induced the Bourbon government, ruling the region at that time, to finance and arrange several ad-hoc surveys. Further, such a calamity was seen as a big challenge by the coeval international scientific community that was engaged in understanding the nature of earthquakes. Therefore, a number of additional investigations were carried out in the first years after the tragedy by scholars and travelers from different countries (see notes about the mainshock in Guidoboni et al., 2007). The overall result of these observations and research activities that is relevant for our study is that a description of the tsunami source and of the tsunami consequences was made available for future generations (see the discussion in Zaniboni et al., 2016).

In this work, the attention is focused on the tsunami impact outside the surroundings of Scilla. The most relevant reported effects are listed in Table 1 and are mainly gathered from recent papers that quote historical sources (i.e. Graziani et al., 2006; Gerardi et al., 2008; the Italian tsunami catalog by Tinti et al., 2007). The last column includes, among others, the main coeval references. The affected locations are shown in Figure 2.

From Table 1, one can observe that the effects of the tsunami were much less in the neighboring area than in Scilla. This is not surprising since it is typical of landslide-tsunamis to attenuate rapidly with distance (see for example Masson et al., 2006; Harbitz et al., 2013, and references therein). However, remarkably the waves were seen in Calabria from Nicotera (point 1,

Figure 2), about 40 km north-east of Scilla, to Reggio Calabria (point 5, Figure 2), 20 km south-west. On the other side of the Messina Straits, the place closest to the source is the easternmost part of Sicily, that is Capo Peloro (point 6, Figure 2), next to the village of Torre Faro (point 7). Here the tsunami was strong and disastrous. In addition to historical sources, the impact of high-energy tsunami waves in this area was confirmed by recent geological investigations carried out in a site called Torre degli Inglesi (Capo Peloro, point 6), about 40 m far from the modern shoreline, where a 15 cm thick sand deposit in a trench layer sequence was attributed to the 1783 event (Pantosti et al., 2008).

Table 1. Summary of pieces of evidence of the 6th February 1783 tsunami in Calabria and Sicily, with the exclusion of local effects in the area of Scilla. For geographic locations, see Figure 2.

| Region	n.	Toponym	Description of the effects	Inundation distance (m)	Run-Up (m)	References
Calabria	1	Nicotera	The sea withdrew and then inundated the beach carrying some fishing boats onshore.			*De Leone, 1783*
	2	Bagnara	Affected by the inundation.			*Minasi, 1785* *De Lorenzo, 1877*
	3	Cannitello	Affected by the inundation.	50	2.9	*Minasi, 1785* *De Lorenzo, 1877*
	4	Punta del Pezzo	Sea covered the beach by one and a half mile, leaving sand on the ground.			*Sarconi, 1784*
	5	Reggio Calabria	The sea inundated the shore carrying a lot of heavy material.	80	3.2	*Torcia, 1783* *De Leone, 1783*
Sicily	6	Capo Peloro	Flooding affected cultivated fields close to the small lake called Pantano Piccolo. Small houses, people and animals were carried seaward. Tsunami deposits identified at Torre degli Inglesi.	>600	6	*Augusti, 1783* *Torcia, 1783* *Gallo, 1784* *Pantosti et al., 2008*
	7	Torre Faro	Tsunami waves flooded the shore, depositing a large amount of silt and a lot of dead fish. Some boats were carried seaward. 26 people drowned.			*Sarconi, 1784* *Torcia, 1783* *Vivenzio, 1788*
	8	Messina	The sea was seen to rise and to noisily inundate the coast. Waves were also quite relevant at the headlight. Sea level rising by about 2 m, reached the fish market, killing 28 people.	50	2	*Minasi, 1785* *Vivenzio, 1783* *Spallanzani, 1795*
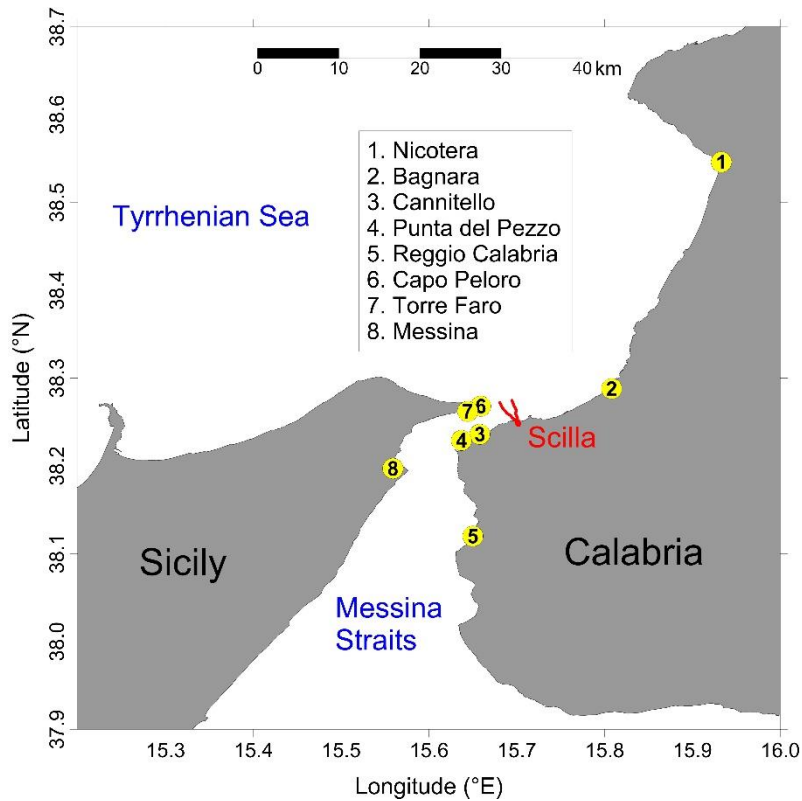
Figure 2. Toponyms reported in Table 1 (yellow circles). The area swept by the 1783 landslide is delimited in red.

3. Numerical Methods

The numerical procedure and techniques used in this paper were developed by some of the authors and presented in previous
5   applications (see e.g. Tinti et al., 2011; Argnani et al., 2012; Zaniboni et al., 2013; Ceramicola et al., 2014; Zaniboni et al., 2014a, 2014b, 2014c; Zaniboni et al., 2016). Therefore, only a brief description will be given here, since the reader can refer to the quoted papers.

3.1 The landslide motion

The numerical code to simulate the landslide motion, UBO-BLOCK1, adopts a Lagrangian approach. The mass is
10   partitioned into a chain of contiguous blocks, and their centers of mass (CoM) are taken as representative points of the landslide. Blocks are allowed to change shape (length, width, and height, the last one influencing strongly tsunami generation) depending on material rheology, while the total volume is conserved. Bulk (gravity, buoyancy) and surface (bottom friction, drag) forces acting on the blocks are accounted for, together with a block-block interaction governed by some parameters that regulate the sliding behavior during the descent. More details can be found in the aforementioned
15   applications, and in the original description given in Tinti et al. (1997).

3.2 Tsunami generation and propagation

The propagation of the waves induced by the landslide moving underwater is modeled through the Navier-Stokes equations in the nonlinear shallow-water approximation and is solved by the code UBO-TSUFD by means of a finite-difference scheme over a regular grid covering the domain of interest. An intermediate code, UBO-TSUIMP, provides a mapping between the Lagrangian and Eulerian grids (used respectively by the codes UBO-BLOCK1 and UBO-TSUFD). Furthermore, it computes the instantaneous tsunamigenic impulse transferring the sea bottom perturbation due to the landslide to the sea surface by means of an appropriate filter function. This term, time-dependent, is included in the hydrodynamic equations as a source term. The tsunami simulation code accounts also for coastal inundation. This is accomplished by adopting the moving boundary technique (the instantaneous shoreline being identified as the dynamic boundary between wet and dry cells), and by using a two-flow grid nesting scheme where a higher resolution is needed. This is usually the case in near-shore regions to obtain accurate inundation results. An extended description of the model UBO-TSUFD can be found in Tinti and Tonini (2013).

4. The landslide simulation

4.1 Scenario reconstruction

The surveys carried out soon after the 1783 event described a wide scar along the Mt. Pacì flank, 1 km west of Scilla, that is still visible today (see Figure 1, yellow contour). Minasi (1785) reported a mass failure starting from 425 m a.s.l. and a landslide front penetrating 100 m into the sea. A later source (De Lorenzo, 1895) mentioned a bigger mass with a larger front (up to 2 km), but a similar offshore mass penetration.

Modern studies performed by means of geophysical surveys and numerical modeling seem to reinforce the hypothesis of a purely subaerial event, though some elements suggest the possibility of a subaerial-submarine collapse. Interpreting land and submarine survey data, Bosman et al. (2006) proved that the scar continues underwater, at least down to 100 m depth. This feature is reported also in Casalbore et al. (2014) and can be seen as evidence that the landslide involved also a submarine failure. However, it can alternatively be interpreted as the effect of the erosion of the sliding surface by the motion of a purely subaerial mass, which is the picture we adopted in the previous paper (Zaniboni et al., 2016) and we maintain herein. Further, it is worth mentioning that Bozzano et al. (2011) applied a stress-strain numerical model to evaluate the response of the Mt. Pacì slope to the shaking of the 5th and 6th February earthquakes and concluded that, though the slide scar admittedly extends underwater, the tsunamigenic source was a purely subaerial collapse, with toe located at about 150 m a.s.l., involving a volume of 5.4 million m^3. They commented that the extension of the scar beyond the initial slide foot might be explained in two ways: either it was the effect of the already cited erosion, produced by the sliding material on the soft surface sediments nearshore, or it was due to a minor submarine failure that occurred before the main slide. Further, Mazzanti and Bozzano, (2011) using an oversimplified single-block landslide model simulated the subaerial tsunami

scenario. Avolio et al. (2009) used cellular automata to simulate subaerial and submarine landslide dynamics, without paying attention to the generated tsunami.

As regards the landslide deposit offshore, it is sufficient to mention that various submarine surveys found an underwater blocky deposit at about 300 m b.s.l. (see Figure 1, dashed red contour), located less than 2 km far from the coast, and associated it to the 1783 slide. The area covered by the deposit is around 700,000 m^2 and can be delimited with a certain degree of accuracy (see Mazzanti and Bozzano, 2011). The total volume is, however, difficult to assess. According to Bozzano et al. (2011), it is compatible with the subaerial scenario landslide; instead, Casalbore et al. (2014) estimated it in the range of 6-8 million m^3.

For the sake of completeness, we mention also that the 1783 Scilla landslide evolution has been the object of a recent application (Wang et al., 2019), where the same subaerial slide scenario has been investigated mainly to test a new numerical method to compute the landslide motion based on a Eulerian fluid solver, using a second-order central scheme with a minmod-like limiter: in the paper the final deposit was used as a constraint to test the accuracy of the landslide simulations, with no attention given to the generated tsunami.

4.2 Results and discussion

In this paper, we make use of the same landslide simulation illustrated by Zaniboni et al. (2016). It is therefore sufficient to synthesize here only the main features of the landslide motion as reported in Figure 3.

The sliding body (upper panel, in blue), reconstructed by considering that the crown is placed at about 400 m a.s.l. and the toe is close to the coastline, results into a subaerial volume of over 6 million m^3, with a maximum thickness of about 100 m in the central part. The main parameter governing the motion is the friction coefficient: in view of the comparison between the final simulated position and the observed deposit boundary, the back-analysis provided the values 0.23 and 0.06 for the subaerial and underwater portions of the slide motion respectively. The red profile in the upper panel of Figure 3 shows the simulated deposit at about 300 m depth.

The middle and lower panels of Figure 3 show the acceleration and velocity of the CoM of the landslide blocks (black dots) as a function of the distance along the profile, together with the average values (green line). Observe that the initial positive acceleration phase, with values around 3 m/s^2, is limited to the subaerial part of the motion (the first 700 m of the profile approximately), while, once underwater, the acceleration adjusts around slightly negative constant values, entailing a slow uniform deceleration phase. This is confirmed by the velocity profile: the average velocity peak is reached just before the entrance of the mass into the water. Notice also that all the CoMs have a similar velocity evolution with distance. The mass has an initial length of around 700 m. For most blocks, the runout is about 2 km, with the exception of the frontal one that travels more than 2.2 km, which results in a lengthening of the slide by about 200 m

7
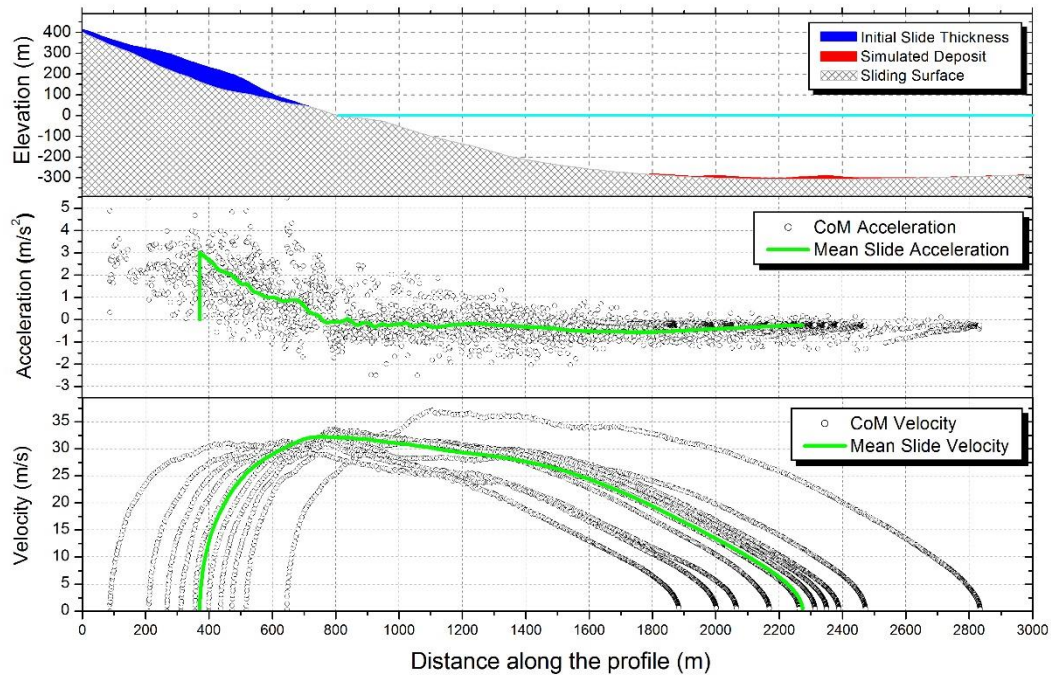
Figure 3. Scilla 1783 slide simulation by means of the code UBO-BLOCK1. Upper Panel: profile of the initial sliding body (in blue) and of the final simulated deposit at about 300 m depth (in red) over the undisturbed sliding surface (grey area). In light blue the sea level. Middle panel: acceleration of the individual CoMs (black circles) and of the CoM of the whole slide (green line) vs. distance along the sliding profile. Lower panel: CoM velocities (black dots) and average velocity (green line) plotted on the sliding track distance.

## 5. Tsunami propagation and impact on the coast

The first step of tsunami simulations is the assemblage of the computational grids, the area covered and the adopted grid resolution depending deeply on the goal of the simulation. In general, the higher the grid resolution, the more accurate are the results, but also the heavier is the related computational effort. The tsunami simulations in Zaniboni et al. (2016) were concentrated in the town of Scilla, and the extent of the very local regular mesh was of a few kilometers in length and width with 10-m spaced nodes (see Grid 1, in green, Figure 4).

In this work, our purpose is two-fold, namely: i) to compute tsunami propagation on a wider area, involving tens of km of Calabria and Sicily coasts, and ii) to compute detailed inundation in the specific area of Capo Peloro, located in front of Scilla. For the first goal, we have built a lower resolution grid (50-m space step) denoted in Figure 4 in red as Grid 2, by using three different databases: SRTM for topography (about 90 m spaced, Jarvis et al., 2008); EMODnet DTM, in its 2018 version, providing bathymetry every ~160 m; and the nautical chart N.138 from Istituto Idrografico della Marina. For this latter case, we have digitized isolines with the aim of characterizing better the shallow water area, not adequately described by previous datasets. The resulting computational mesh covers an area of 30x27 km^2. As concerns the Calabria coast, it runs

8

from Bagnara, 10 km west of Scilla to Reggio Calabria, about 20 km south-westward. Regarding Sicily, the grid includes the city of Messina and 7-8 kilometers of coast southward as well as a piece of the northern coast facing the Tyrrhenian Sea by an extension of at least 10 km.

The choice of Capo Peloro as the target area for the grid resolution enhancement will be justified later, in the discussion of the simulation results obtained on the coarser domain. Figure 4 illustrates the extent of Grid 3 and 4 (how they differ from one another will be explained later as well) in blue, that are actually a westward extension of Grid 1 with the same spatial resolution (10 m).

Before discussing the simulation results, it is worth providing some terminological specifications: with "wave height" or "wave elevation" offshore, we mean the difference between the offshore water top and the mean sea level; the "flow depth" is the height of the water with respect to the ground, onshore; consequently, the onshore "wave height" is the sum of flow depth and local topographic level; final, with "runup" and "inundation distance" we denote the maximum onshore ground elevation and the maximum onshore penetration (approximately normal to the shore) reached by the tsunami, respectively.
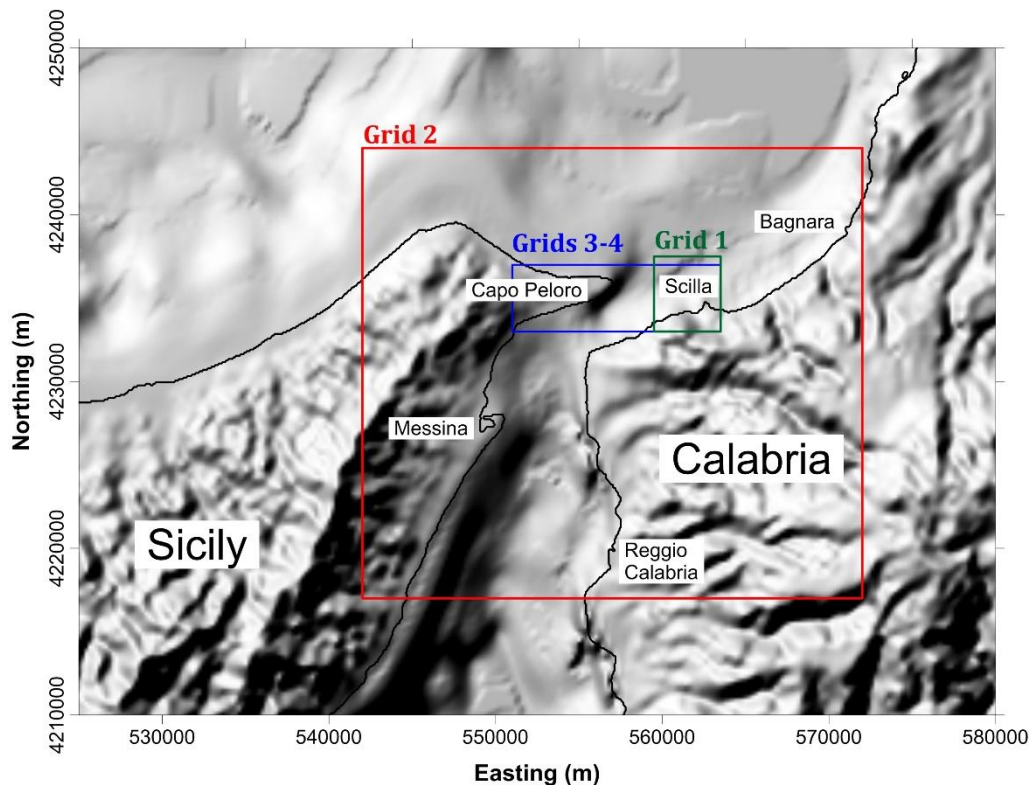
Figure 4. Computational grids adopted for numerical simulations of tsunami propagation: Grid 1 (green) was used for the tsunami simulations by Zaniboni et al. (2016); Grid 2 (in red) has been used in the first simulation of this paper; Grid 3 and 4 (in blue) are an extension of Grid 1 covering the target area of Capo Peloro. Coordinates are in UTM-WGS84 projection, zone 33N.

5.1 Simulation over the 50 m-spaced grid

Figure 5 shows the maximum water elevation, obtained by considering the maximum value of the sea surface height reached during the simulation time span in each node of Grid 2. This category of plots provides a general spatial pattern of the tsunami energy distribution that, in the intermediate and far-field depends more on the bathymetry than on the source type. Therefore, it allows one to distinguish the areas that are more prone to tsunami attacks.

The area close to the slide shows, as expected, the highest water elevations with more than 8 m in Scilla and waves at least 4 m high (in red) affecting the surroundings coast for about 6 km. The wave height distribution illustrated in Figure 5 provides also indications on the extension of the coast affected by 1.5 to 2 m (in yellow), and 1 m maximum wave (in green), resulting in approximately 10 km and 20 km respectively along the Calabrian coasts. South-westward, in the Messina Strait, the maximum height reaches 0.5 m.
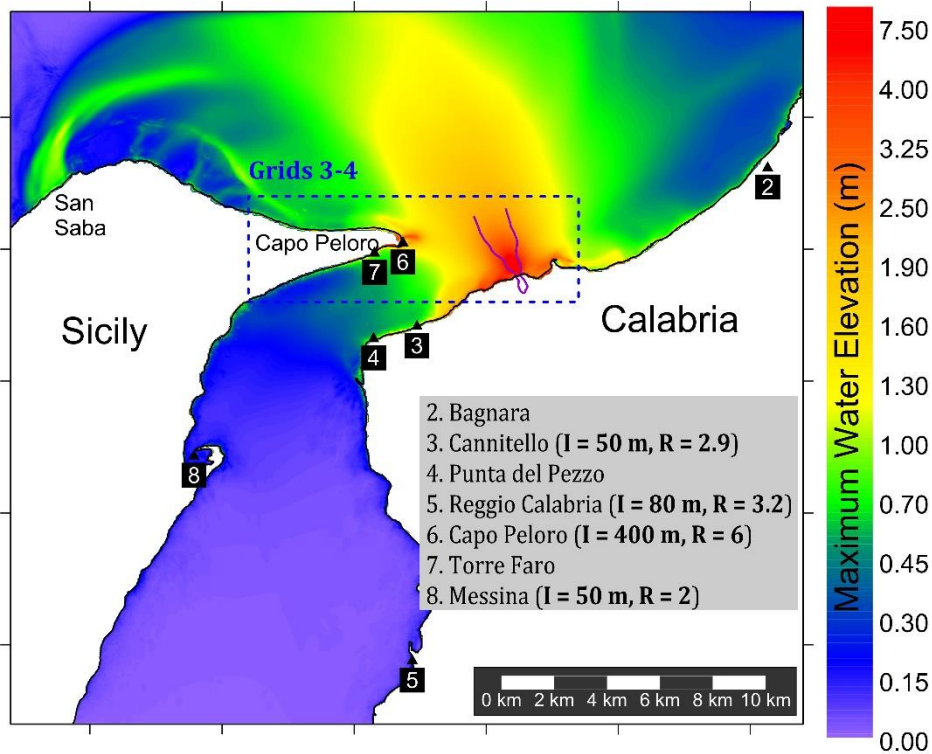
Figure 5. Maximum tsunami elevation, computed for each point of Grid 2. Numbers represent the positions of the available observations (see Table 1). The respective toponyms are reported in the legend together with the observed inundation distance (I) and runup (R). The blue dashed rectangle marks the limits of the 10 m resolution Grids 3 and 4, zooming on the area of Capo Peloro, that differ from one another only for a small part of their topography. The purple boundary delimits the sliding surface of the 1783 Scilla landslide. For geographical coordinates see Figure 4.

Moving to the coast of Sicily, especially north of the Messina Strait, some significant features are observed. First, a strong tsunami energy concentration can be noted towards the easternmost end of Sicily, named Capo Peloro, where waves higher

than 6 m hit the coastline. Along the Tyrrhenian coast of Sicily other tsunami beams are clearly visible (in green, meaning at least 1 m height), the most interesting of which is the western one, affecting the coastal area close to the small village of San Saba. Overall, the simulation confirms the generally known feature that for landslide-tsunamis the wave height decays rapidly with distance.

5   When comparing the simulation results with the observed effects a general underestimation can be noticed: for example, in point 3 (Cannitello) of the map of Figure 5 a runup of 2.9 m has been reported, higher than the 1 m maximum height obtained in the simulation. The same holds for Messina (#8) and Reggio Calabria (#5), the most important towns in the Messina Strait, where the difference is by far bigger. Only the area of Capo Peloro (#6 and #7) seems to fit the observations. Such discrepancies can be ascribed to the low resolution of the computational domain (50 meters) not allowing one to

10   describe properly the coastal zone and all the non-linear effects prevailing in shallow water, such as the inland inundation. Further, low-resolution simulations often cannot account for tsunami wave amplification caused by resonances induced inside coastal basins, such as harbors (see for example Dong at al., 2010; Vela et al., 2010). This latter can explain, for example, the underestimations of the observations reported in Messina and Reggio Calabria.

These considerations push to the use of a more detailed computational grid for the sites of major interest, suggesting that the

15   optimal approach is: 1) to assess the general tsunami energy distribution in the first run of simulations carried out in a wider low-resolution domain 2) to pick up the areas most exposed to tsunami attack (e.g. areas hit by energy beams) to perform higher-resolution investigations. With this approach in mind, the focus has been moved to the area enclosed in the blue-dashed rectangle of Figure 5, including Capo Peloro, where most of the devastating effects of the tsunami outside the source zone were reported (see Table 1, #6 and #7).

20   **5.2 First tsunami simulation in the Capo Peloro area**

An additional computational grid (Grid 3) has then been built to simulate the tsunami propagation and inundation in this zone.

In this application, actually, due to the proximity of the landslide to the target area, the choice was to build Grid 3 by extending westward the high-resolution grid (Grid 1, 10 m node spacing) used by Zaniboni et al. (2016) for the simulation of

25   the local tsunami effects in Scilla. The relevant data for the Sicilian region was provided by the Civil Protection Department of Sicily and retrieved from the regional cartography service, SITR (Sistema Informativo Territoriale Regionale) in the form of a DTM describing the present topography of the coastal zone with high detail. As for bathymetric data, they have been retrieved from the same sources used for Grid 2. Grid 3 covers an area of 12.5 km (E-W) by 4 km (N-S), for a total of more than 500,000 nodes. As can be noticed from the map in Figure 6, the Capo Peloro presents a morphology that is radically

30   different from the Calabrian coasts. In Calabria coasts are steep, rapidly ascending to 400 m a.s.l., while in the area of Capo Peloro a wide lowland is found, extending for about 2x1 km with elevation in the order of 1 to 5 meters. This area is now densely inhabited, with many houses facing the sea especially along the southern coast. Another interesting feature is the presence of two brackish lakes, called Ganzirri Lake and Pantano Piccolo (also known as Faro Lake), characterized by 6 m

and 29 m water depth respectively. They are connected to the sea (and to each other) by narrow channels, built under the English authority at the beginning of XIX century (Leonardi et al., 2009; Manganaro et al., 2011; Ferrarin et al., 2013). One of the most relevant observations reported in the historical reconstruction of the tsunami effects is that the basin of Pantano Piccolo was reached by the sea water in 1783 (Minasi, 1785). This feature should be considered in the evaluation of the simulated tsunami accuracy.
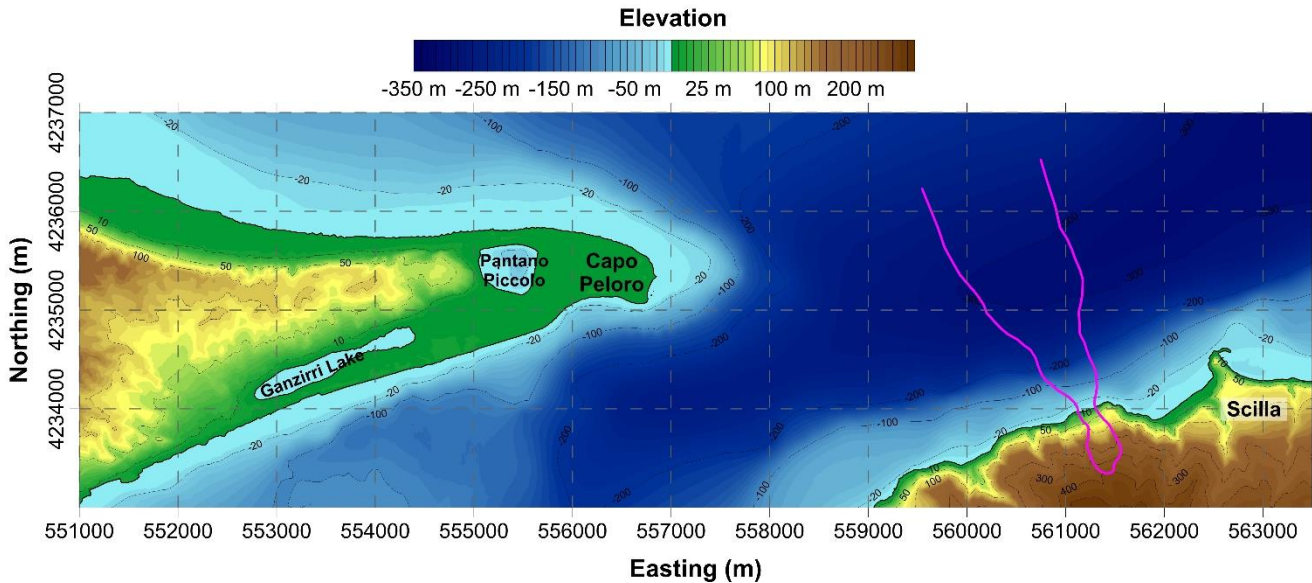

Figure 6. Area covered by Grids 3 and 4 employed to simulate the impact of the 1783 tsunami in Capo Peloro, the easternmost point of Sicily. The magenta contour delimits the strip swept by the landslide. Coordinates are in UTM-WGS84 projection, zone 33N.

Figure 7 shows different frames of the tsunami propagation simulated by means of the code UBO-TSUFD, starting from the snapshot taken at 80 seconds. It is worth pointing out that the origin time coincides with the landslide motion initiation and recalling that, according to our simulation, the slide enters the sea between 10 and 30 seconds, and settles at the final position around 110 s (see Zaniboni et al., 2016, for the accurate description of these results).

The landslide-generated wave heads towards Capo Peloro with a strong positive front 5 m high, directly originated by the slide entering the sea and characterized by an almost circular shape when moving in deep water. At t=100 s the wave begins changing form, due to the interaction with the platform characterizing the seabed east of Capo Peloro. When meeting shallow water, the tsunami is intensely decelerated and begins to deform. Frames at 100 s, 110 s and 120 s display the subdivision of the wave into two fronts, north and south of the Capo Peloro end, attacking the coast obliquely. At 140 s the southern coast of the cape is reached by the tsunami, that floods the mainland by some tens of meters, and then inundates the other parts. In the eastern extreme the water penetration is maximum, reaching 600-700 m distance (as visible from the 200 s frame). At the same time, the northern branch of the tsunami reaches the coastline with a positive 2 m high front that tends to align to a direction parallel to the shoreline. The following oscillations constituting the train of waves (already visible behind

12

the tsunami front in the first snapshots) do not produce relevant effects on the coast, apart from the cape, where a second relevant positive signal, exceeding 2 m, can be noticed at t=240 s.
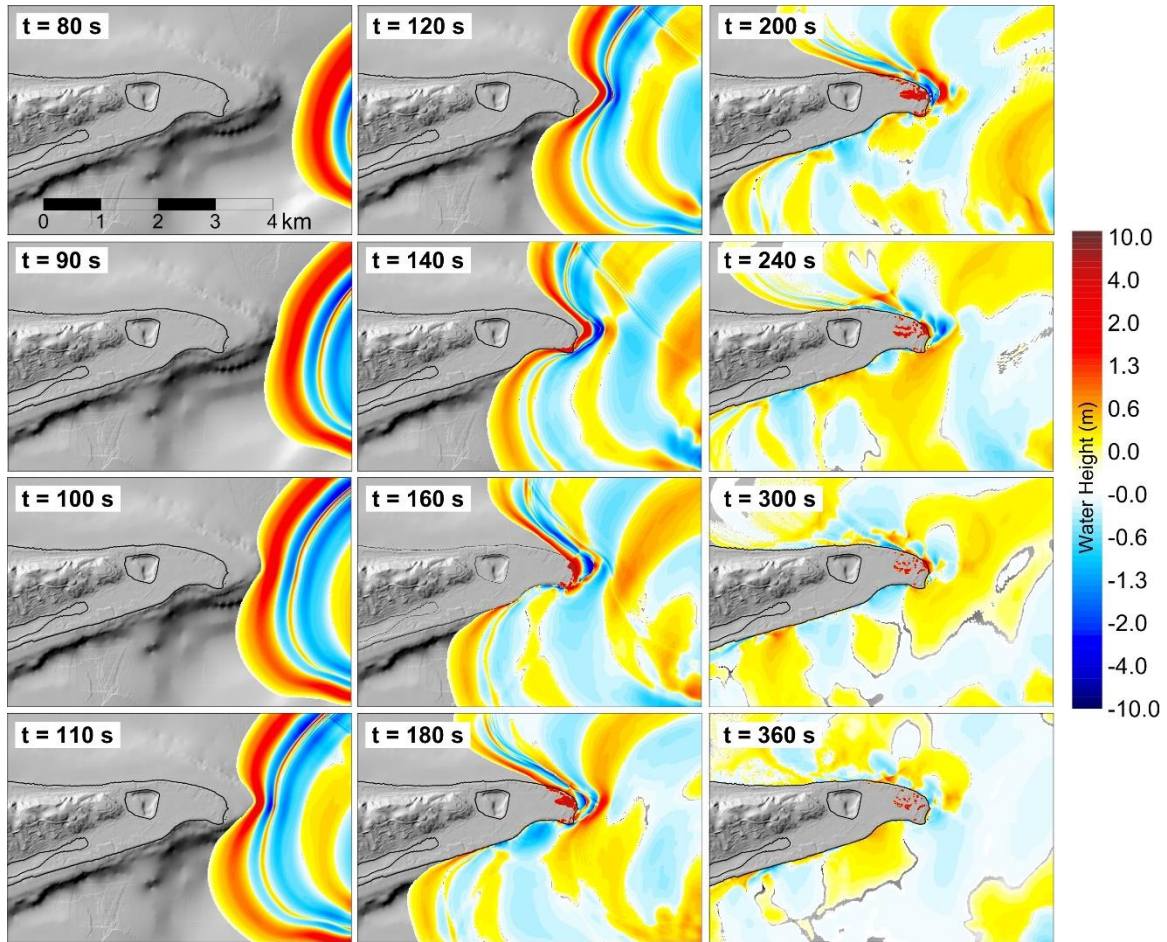

5

Figure 7. Propagation frames for the 1783 Scilla landslide-tsunami in the target area of Capo Peloro, eastern Sicily. Geographical coordinates in Figure 6.

The maximum water elevation for each node of the western portion of Grid 3 is illustrated in Figure 8. Some of the features already observed in the 50 m grid (#2, see Figure 5) are confirmed, such as the maximum wave height concentration in the
10   easternmost zone of Capo Peloro. Here, in correspondence with the edifice named Torre degli Inglesi ("English Tower", referring to a building realized during the English domination, marked in black in Figure 8), some tsunami deposits were recognized and associated to the 1783 event (Pantosti et al., 2008). The simulation shows exactly for this spot the maximum water elevation, exceeding 6 m, and the maximum inland penetration, more than 700 m. Furthermore, here one can notice the main discrepancy between the low-resolution Grid 2 and the high-resolution Grid 3 simulations: in the former case, only

a few inland cells (purple in Figure 8) are inundated (corresponding to an inundation distance of 150 m), while in the latter the inland penetration is by far larger. For the remaining coastal stretch, the water flooding is limited to some tens of meters or less, showing little differences between the two simulations. It is very relevant to stress that, concerning the small lake of Pantano Piccolo, both simulations exclude that it is reached by the tsunami, contrary to what reported in the historical reconstructions.
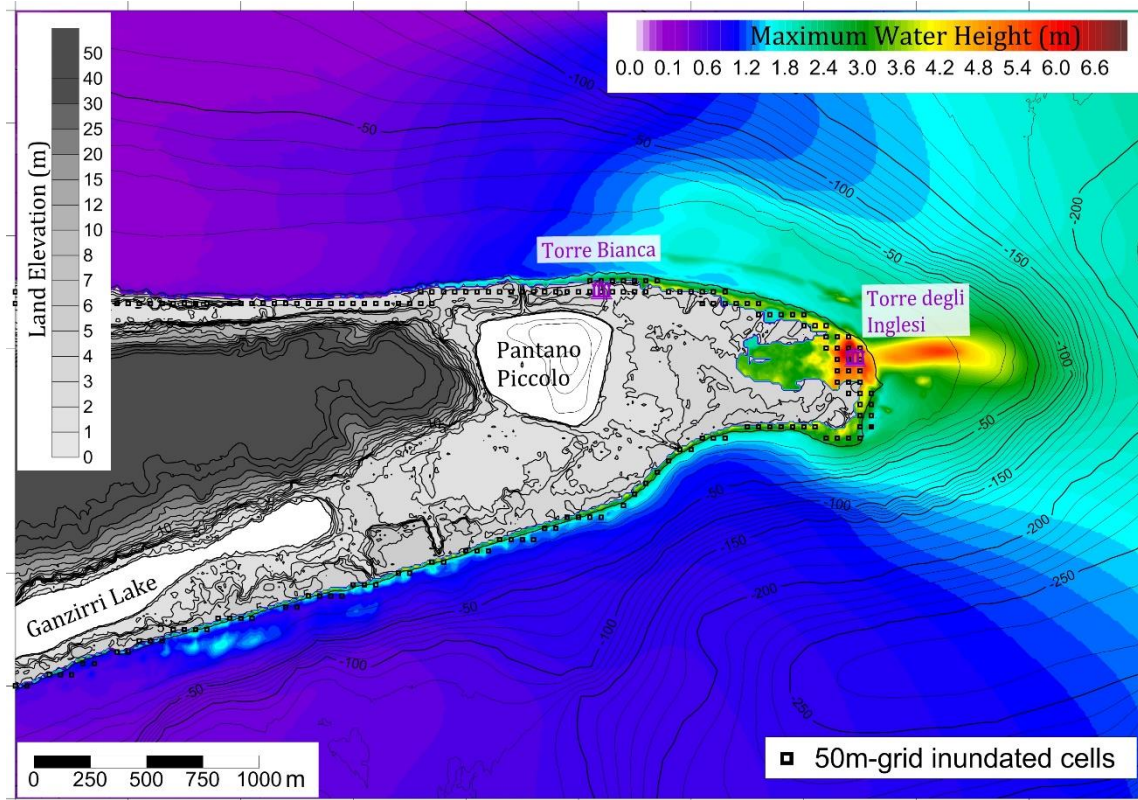
Figure 8. Maximum water inundation in Capo Peloro for the high-resolution Grid 3 (western portion). The black squares mark the cells inundated in the simulation with the low-resolution Grid 2. The purple symbols represent the positions of historical buildings: Torre degli Inglesi, the site where tsunami deposits were recognized and associated with the 1783 event (Pantosti et al., 2008); Torre Bianca, partially buried by sand deposits (Bottari and Carveni, 2009). For geographical coordinates see Figure 6.

6. Capo Peloro: morphology reconsideration

The transition from Grid 2 to Grid 3 produced interesting results and precious insights on the tsunami effects in the target area. Yet, as already noted, one of the most relevant features (i.e. the inundation of the lake of Pantano Piccolo) was not reproduced, nor the uncertainties naturally connected with the simulation of natural events like landslides and tsunamis can be invoked. Indeed, to generate a tsunami able to penetrate further the flat area beyond Torre degli Inglesi and to cover the distance of more than 2 km separating this from the lake, a much larger landslide should be needed, which is against the

14

geological evidence. Another possibility would be that the tsunami finds a penetration way from other directions, for example from the north. In fact, the strip of land between the basin and the sea is narrow (around 150 m) and is characterized by 3 to 5-meter topography, again really unlikely to be overrun by the simulated tsunami.

A possible alternative solution comes from the considerations on the coastal morphology of this area. In a historical study of this zone, Randazzo et al. (2014) gave evidence of the strong variability of the coastal stretch around Capo Peloro, due to the action of atmospheric agents. The dataset used to build Grid 3 refers to the present ground level, that can have experienced great changes since the 1783 event. Based on the historical investigations by Bottari et al. (2006) and Bottari and Carveni (2009), we know that in Pantano Piccolo some hundreds of ships took shelter during the early Roman period (5th century B.C.), and that probably also a small harbor existed, meaning the presence of direct access from the sea. In the following centuries the channel was filled with sediments, but a look at the topography clearly shows that the lower ground area starts from the north-eastern corner of the lake (as evidenced also by the modern 2-m isoline taken from Bottari et al, 2006), and is the best candidate for the channel that was connecting the lake to the sea more than two thousand years ago. Currently, the access is closed by a 3-4 m sand dune on the coast, that can be reasonably associated to progressive sedimentation due to wind and storms and removed, in order to reconstruct a tentative 1783 morphology of the area.

Another element that needs to be considered is the existence, on the narrow coastal stretch separating Pantano Piccolo from the Tyrrhenian Sea, of a partially buried tower named Torre Bianca ("White Tower", known also as "Mazzone", see Figures 8 and 9 for location), that now is filled with sand up to the first floor (Bottari and Carveni, 2009). Yet in the XVIII century, this building served as a storehouse, so probably fully available and unburied, meaning that the previously cited assumption of removing 3-4 m of sediments (corresponding to the average height of one floor) in this area is perfectly reasonable.

Keeping all these considerations in mind, a rearrangement of Grid 3 has been done resulting in a new mesh, the Grid 4, with the same spatial extension. Figure 9 shows in the upper panel a shaded-relief map of the present topography and bathymetry, and the corrections that have been done to reconstruct the likely morphology of 1783. Notice again that in Figure 9 only the western portions of Grid 3 and 4, covering the target area, are reported, since the source area remained unchanged. Such reconstruction is based on hypotheses and some evidence. For example, the two small channels now connecting Pantano Piccolo to the sea did not exist in 1783, since they were excavated during the following English domination. For this reason, they have been "filled" in Grid 4. The most relevant changes, regarding the area between the north-east corner of Pantano Piccolo and the Torre Bianca site, is the removal of 1 to 5 m of the surface ground layer. The highest amount of "digging" is located close to the coast, where the sand dune currently closing the possible access of water (and presumably filling the first floor of Torre Bianca) has been leveled. Morphological changes in other areas of the cape are much less realistic since they would entail lowering of high topography that is less intensely affected by natural agents such as storms, winds or sea waves.
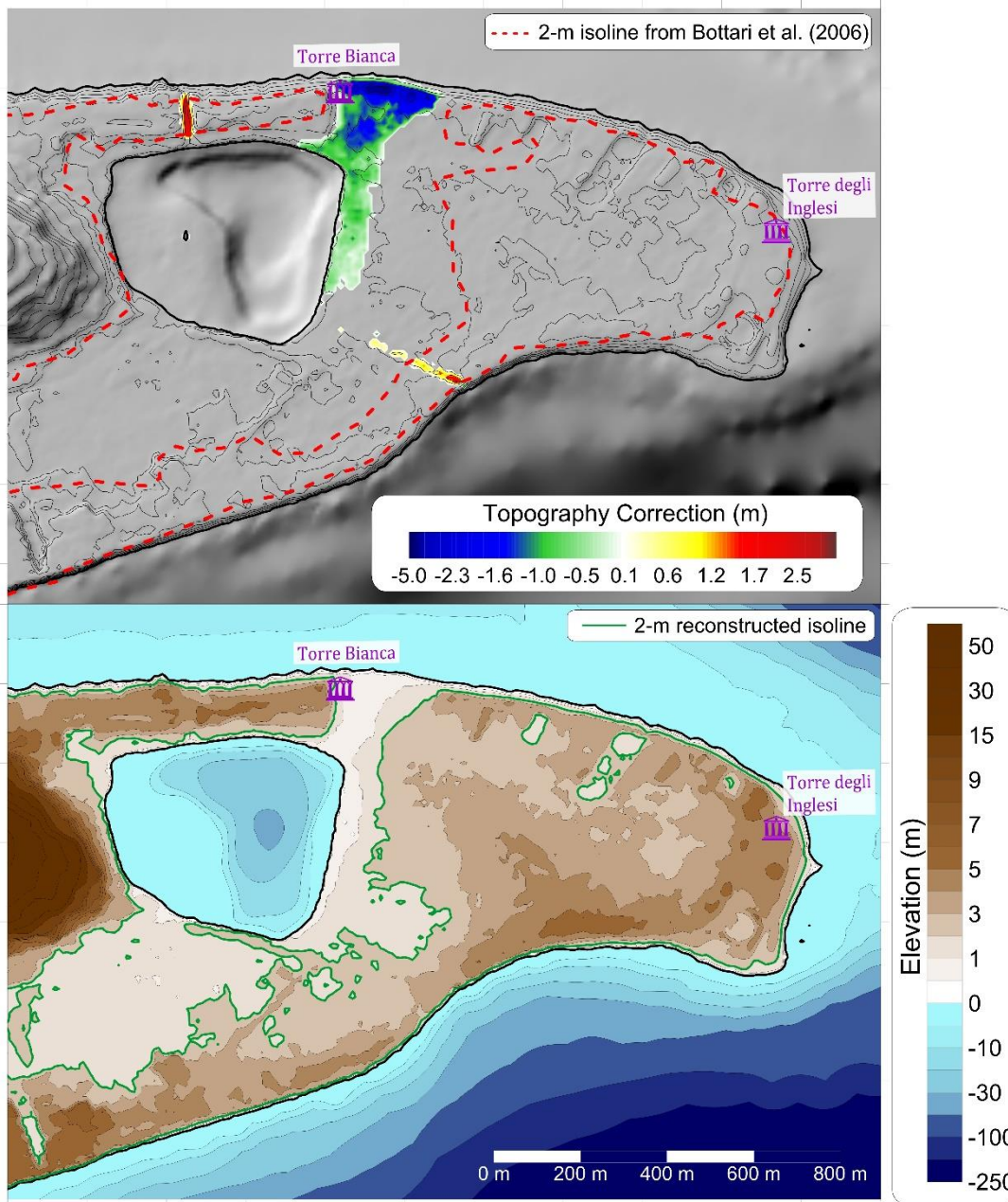
Figure 9. Upper panel: Shaded-relief map of the current topography of Capo Peloro, with 2-m isoline (red-dashed line) obtained from Bottari et al. (2006) showing the most likely connection between the lake and the sea, just east of Torre Bianca. The corrections are shown in green-blue when negative (meaning "digging" with respect to the present ground level) and in yellow-red when positive, meaning increased ground elevation. Lower panel: Contour plot of Grid 4, with the low topography from the northeastern corner of the lake to the sea. In green, the new 2-m isoline is evidenced. With the corrected topo-bathymetry we have built the Grid 4 that has the same areal coverage as Grid 3. For geographical reference, see Figure 6.

16

The tsunami simulation in Grid 4 coincides with the simulation in Grid 3 for the first 200 seconds, as is shown in Figure 10. The main differences start from the 220 s frame, when the coastal area east of Torre Bianca begins to be inundated. The following frames show that the water reaches more than 1 m height, channeling through the modified area and reaching the lake between 240 and 260 s. After that, a small positive wave propagating inside the basin can be noticed, 10 to 20 cm high, with also some reflections. The adopted correction to the topography, then, facilitates the tsunami flooding of the Pantano Piccolo lake.
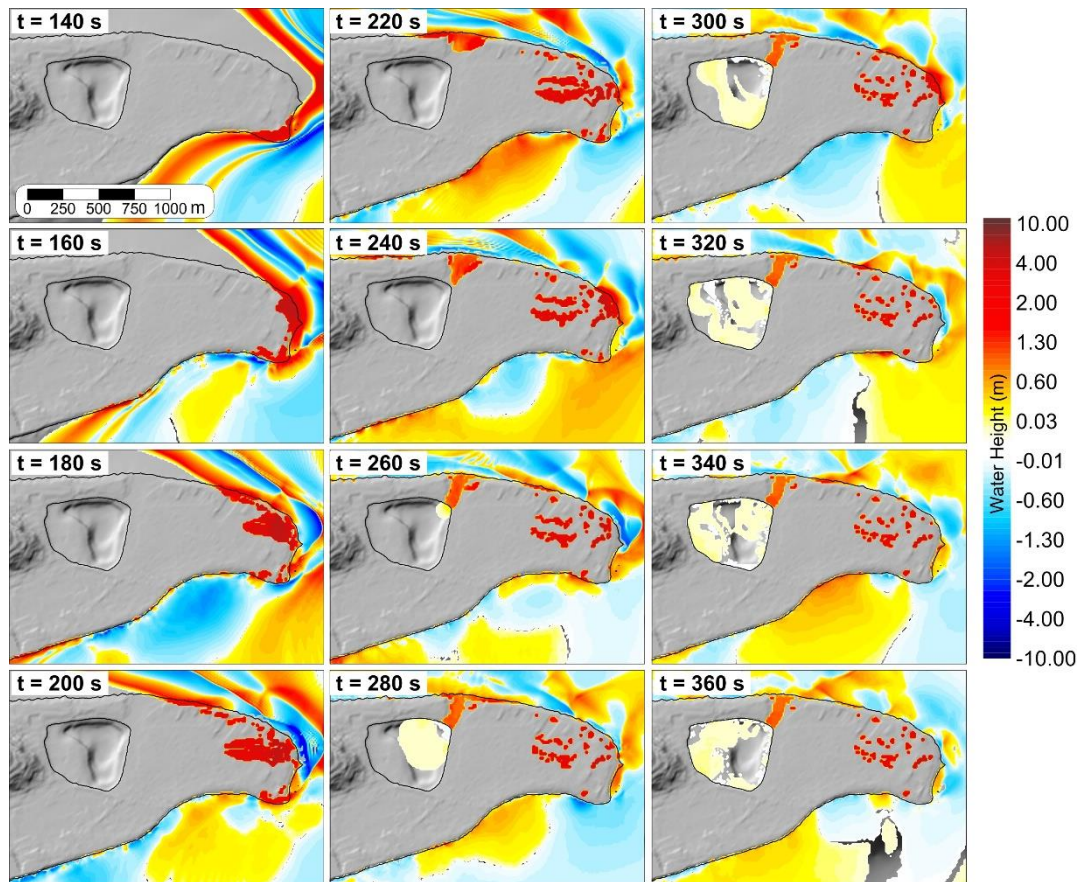

Figure 10. Propagation frames of the 1783 landslide-generated tsunami on the western part of Grid 4. Notice the water propagation inside the lake. Geographical coordinates in Figure 6.

The map with maximum water elevation (Figure 11, upper panel) is analogous to the one of Figure 8. The main difference comes from the modified zone, where the water climbs up to 2.5 m close to the coast and 1 m just before entering the lake. Inside the basin, the maximum wave elevation reaches 40 cm in the western part, but less in the central area, that is deeper. The lower panel displays the height of the water column characterizing the flood, known usually as flow depth. The plot shows that the northern coast is affected by higher flow depth, reaching almost everywhere 2 m, with the maximum located

17

at the Torre degli Inglesi (more than 5 m). The flood, just before entering Pantano, is characterized by a water column of about half a meter.
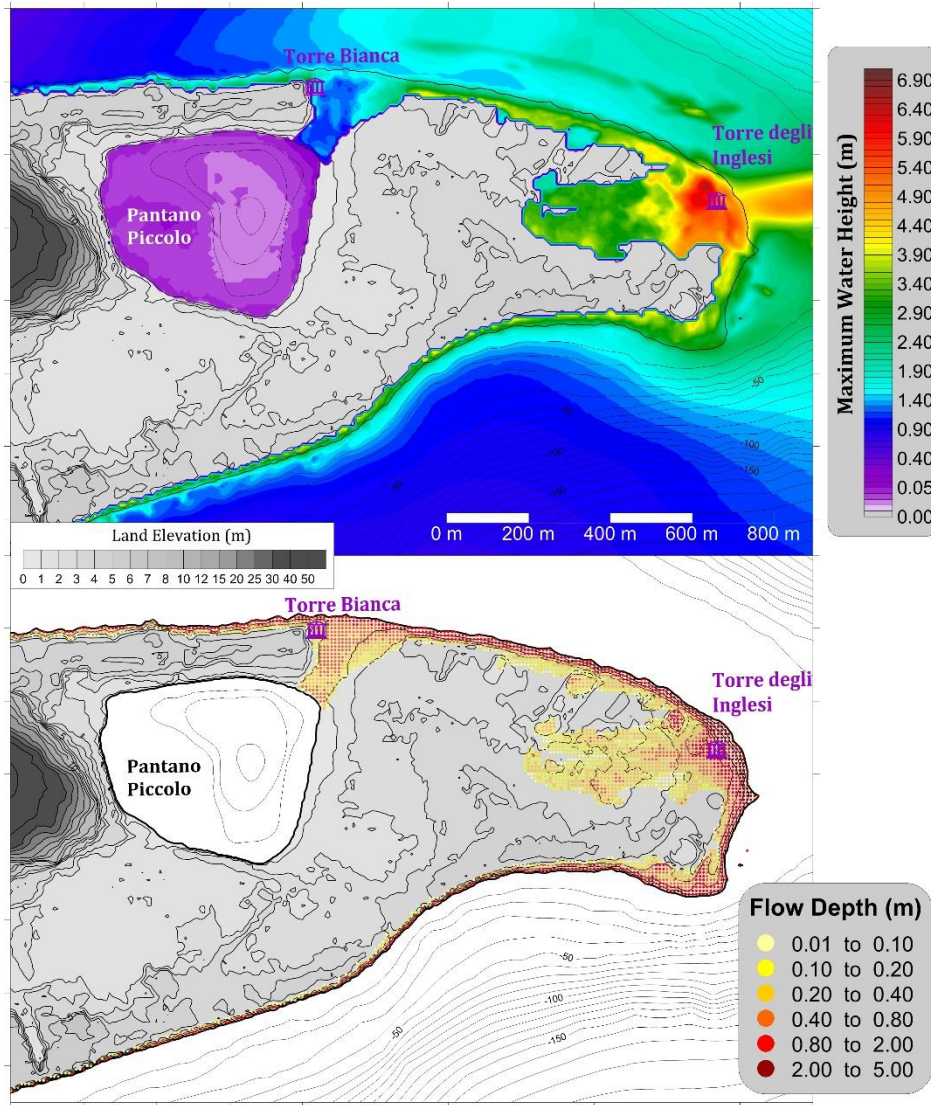
Figure 11. Upper panel: Maximum water elevation for the western part of Grid 4. Notice that tsunami penetrates also into the lake. Lower panel: Maximum flow depth for each topographic node. For geographical coordinates, see Figure 6.

7. General discussion

In this paper we have performed a deep analysis of the 1783 tsunami extending the results of a previous study where attention was restricted to the area of the highest impact, that is Scilla and surroundings. Here, we have simulated the

tsunami in a broader region and we can draw the following remarks. An interesting, yet unexpected feature, we found is the strong tsunami beam reaching the village of San Saba, located along the northern coast of Sicily, 10 km westward (see Figure 5). There is no historical account of a tsunami impact here. But this can be easily explained by considering that probably the tsunami affected only the beach and passed unobserved. As for the Calabria coast, we observe that the

5   simulated wave height rapidly decreases with distance from the tsunami origin, as expected for landslide-induced tsunami events. In addition to the positive results highlighted above, we have also to point out, as a drawback, that in the region covered by the 50-m resolution grid (Grid 2), a general underestimation of the observed wave height is noted, which has to be ascribed to an insufficient description of the local, shallow bathymetry and of the coastal topography features. The conclusion is that 50-m computational domain is suitable to assess the general pattern of the tsunami energy distribution,

10   highlighting the areas where the highest waves concentrate, while is inadequate to provide good coastal tsunami data for the 1783 case.

The area presenting the highest interest is Capo Peloro, the easternmost cape of Sicily, where the most damaging effects besides Scilla were recorded, including a deep tsunami penetration and the death of 26 persons, that is the only life toll of the tsunami away from the source. Thus, this zone has been selected as a good target for a grid refinement. A higher resolution

15   computational domain (Grid 3, 10-m spaced) has been then assembled, based on the present morphology. The tsunami simulation on Grid 3 shows that the inundation distance in the area of maximum impact changes radically, passing from 150 m found for Grid 2 to more than 600 m (Figure 8), in full agreement with the observations. This feature clearly shows the improvement brought by the computational grid adjustment.

However, the tsunami does not reach the Pantano Piccolo lake, which contrasts sound historical accounts (see Minasi, 1785).

20   This misfit calls for simulation changes that can be done with three possible options: i) to produce a stronger tsunami; ii) to use a better resolution; iii) to change the basic topo-bathymetry dataset, especially in the target area. We have excluded option 1, that is to use Grid 3 and to produce a stronger tsunami by using a larger volume landslide, since the landslide geometry is well constrained by geological considerations on the scar morphology and by the identified offshore deposit, and also by the good agreement with observations of the tsunami run-up height in the Scilla beaches computed through Grid 1

25   (see Zaniboni et al., 2016). We have further ruled out also option 2, that is to use grid spacing finer than 10 m, since this resolution was enough for the target area, as mentioned before, and also because it was enough to fit the 600-m observed inundation of Capo Peloro with Grid 3. So the only left option was to keep the same resolution and to build another set, Grid 4, that is based on opening a way to the tsunami access through an ancient channel that was a pathway to an inner well-protected harbor in ancient Roman times, and that is presently filled with sediments and obstructed by a coastal sand dune

30   (Figure 9). The signature of this channel is still recognizable today in a linear topographic depression (only 2 m high a.s.l.) going from the north-eastern corner of the lake to the sea. We believe that Grid 4, allowing the tsunami to reach the lake, represents reasonably well the Capo Peloro topography at the time of the 1783 tsunami occurrence, also based on the existence of Torre Bianca building, whose present status reinforces the plausibility of sand deposit removal along the coast.

The tsunami reached the lake through the channel either because there was no coastal dune, as assumed in Grid 4, or because the dune was lower than today and was overcome and/or demolished by the incoming tsunami.

8. Conclusions

The work presented here is the natural extension of the Zaniboni et al. (2016) paper, where the initial sliding mass (subaerial) was reconstructed, its descent along the Mt. Pacì flank and its immersion in the sea were simulated, and the effects of the generated wave on Marina Grande beach of Scilla (where most of damages and casualties resulted) were assessed. The tsunami simulations were performed in a high-resolution (10 m) grid, covering the town of Scilla (as depicted in Figure 4). Encouraged by the very satisfactory results obtained, well-fitting the detailed historical reports, in this work we have applied the same numerical codes to extend the study of the tsunami to a wider scale.

This has been done by means of additional simulations: one in a wider domain, covering a larger portion of Calabria and the north-eastern Sicily coasts, characterized by a lower resolution (50 m node spacing) and two over a high-resolution domain (10-m spacing), embracing Capo Peloro, where the present topo-bathymetry (Grid 3) and a reconstructed topo-bathymetry (Grid 4) have been used to investigate tsunami flooding.

The simulation over a wider domain provides interesting hints on the tsunami energy distribution on the regional scale, heading mainly towards Capo Peloro, where tsunami effects were strong, according to historical records and study of tsunami deposits. The focus on some areas of interest, realized with grid refinement, allows one to obtain a better fit with the observations. In this particular case, the adjustment of Capo Peloro morphology was necessary to account for the inundation of the small basin of Pantano Piccolo.

This paper together with the previous paper by Zaniboni et al. (2016) provides a good reconstruction of the 1783 landslide-induced event, respecting the main available geological constraints and fitting the tsunami observations in those places where the tsunami was most lethal, namely the areas of Scilla and Capo Peloro (see simulations in Grids 1 and 4).

Still, some level for improvement remains for fitting observations in places covered by Grid 2, which means that probably local high-resolution grids have to be nested, to handle areas where a better agreement has to be searched, as for example in the harbors of Messina and Reggio Calabria. Here probably local effects such as eigenmode resonance strengthened the tsunami waves. But this will be left to further analyses.

A final consideration regards the area of Capo Peloro, that is densely populated with a flat inland topography, and placed in a region with many potential tsunami sources around, either due to earthquakes or to coastal landslides. Hence it needs particular attention in terms of hazard, vulnerability and risk assessments. This paper, through the simulation carried out on Grid 4, has shown the effect of coastal channels as elements favoring tsunami penetration. Since there are today active channels connecting the lake of Pantano Piccolo and Ganzirri to the waters of the Messina Straits, their role should be explored and taken into account when planning and designing civil protection measures.

Authors' Contribution

Filippo Zaniboni reconstructed the landslide scenario, performed the landslide simulation, arranged the tsunami computational grids, prepared the initial draft of the paper and managed the following phases of publication; Gianluca Pagnoni who tests and maintains the tsunami simulation code, helped prepare the tsunami computational grid and contributed to the paper improvement; Glauco Gallotti contributed to the landslide scenario definition and to the paper review and editing; Maria Ausilia Paparo retrieved relevant information on historical reports reconstructing the tsunami effects and contributed to the landslide scenario definition; Alberto Armigliato contributed to computational grid preparation and revised the paper; Stefano Tinti supervised the whole work and reviewed the paper drafts.

Competing interests

The authors declare that they have no conflict of interest.

References

Argnani, A., Armigliato, A., Pagnoni, G., Zaniboni, F., Tinti, S., and Bonazzi, C.: Active tectonics along the submarine slope of south-eastern Sicily and the source of the 11 January 1693 earthquake and tsunami, Nat. Hazards Earth Syst. Sci., 12, 1311–1319, www.nat-hazards-earth-syst-sci.net/12/1311/2012/, doi: 10.5194/nhess-12-1311-2012, 2012.

Augusti, M.: Dei terremoti di Messina e di Calabria dell'anno 1783, memorie e riflessioni, Bologna (in Italian), 1783.

Avolio, M.V., Lupiano, V., Mazzanti, P., and Di Gregorio, S.: A Cellular Automata Model for Flow-like Landslides with Numerical Simulations of Subaerial and Subaqueous Cases. EnviroInfo 2009 (Berlin), Environmental Informatics and Industrial Environmental Protection: Concepts, Methods and Tools. Copyright © Shaker Verlag 2009. ISBN: 978-3-8322-8397-1, 2009.

Bosman, A., Bozzano, F., Chiocci, F.L., and Mazzanti, P.: The 1783 Scilla tsunami: evidences of a submarine landslide as a possible (con?)cause. Geophysical Research Abstracts, Vol. 8, 10558, 2006.

5   Bottari, A., Bottari, C., Carveni, P.: Evidenze dell'antico portus pelori da analisi paleotopografiche della penisola di Capo Peloro (Sicilia Nord-Orientale). Il Quaternario, Italian Journal of Quaternary Sciences, 19(1), 2006 - 167-174, 2006.

Bottari, C., Carveni, P.: Archaeological and historiographical implications of recent uplift of the Peloro Peninsula, NE Sicily. Quaternary Research 72 (2009) 38–46. doi:10.1016/j.yqres.2009.03.004, 2009.

10

Bozzano, F., Lenti, L., Martino, S., Montagna, A., and Paciello A.: Earthquake triggering of landslides in highly jointed rock masses: Reconstruction of the 1783 Scilla rock avalanche (Italy), Geomorphology, 129, 294-308, 2011.

Casalbore, D., Bosman, A., Ridente, D., and Chiocci F.L.: Coastal and Submarine Landslides in the Tectonically-Active

15   Tyrrhenian Calabrian Margin (Southern Italy): Examples and Geohazard Implications, In: Krastel S. et al. (eds) Submarine Mass Movements and Their Consequences, Advances in Natural and Technological Hazards Research, vol 37. Springer, Cham, 2014.

Ceramicola, S., Tinti, S., Zaniboni, F., Praeg, D., Planinsek, P., Pagnoni, G., and Forlin, E.: Reconstruction and tsunami

20   modeling of a submarine landslide on the Ionian margin of Calabria (Mediterranean Sea), K. Sassa, P. Canuti, Y. Yin (eds.), Landslide Science for a Safer Geoenvironment, Vol. 3, pp. 557-562, doi: 10.1007/978-3-319-04996-0_85, © Springer International Publishing Switzerland, 2014.

De Leone, A.: Giornale e notizie de' tremuoti accaduti l'anno 1783 nella provincia di Catanzaro, Napoli, (in Italian), 1783.

25

De Lorenzo, A.: Memorie da servire alla storia sacra e civile di Reggio e delle Calabrie. Cronache e Documenti inediti o rari, Vol. I, Reggio Calabria (in Italian), 1877.

De Lorenzo, A: Un secondo manipolo di monografie e memorie reggine e calabresi, Siena (in Italian), 1895.

30

Dong, G., Wang, G., Ma, X., and Ma, Y.: Harbor resonance induced by subaerial landslide-generated impact waves, Ocean Engineering, 37, 927–934, 2010.

EMODnet Bathymetry Consortium (2018): EMODnet Digital Bathymetry (DTM). http://doi.org/10.12770/18ff0d48-b203-4a65-94a9-5fd8b0ec35f6

Ferrarin, C., Bergamasco, A., Umgiesser, G., Cucco, A.: Hydrodynamics and spatial zonation of the Capo Peloro coastal system (Sicily) through 3-D numerical modeling. Journal of Marine Systems 117–118 (2013) 96–107. DOI: 10.1016/j.jmarsys.2013.02.005, 2013.

Gallo, A.: Lettera istorico-fisica de' terremoti accaduti in Messina nel mese di febbraio di quest'anno 1783, Messina, 8 marzo 1783, Bologna (in Italian), 1784.

Gerardi, F., Barbano, M. S., De Martini, P. M., and Pantosti, D: Discrimination of Tsunami Sources (Earthquake versus Landslide) on the Basis of Historical Data in Eastern Sicily and Southern Calabria, Bulletin of the Seismological Society of America, Vol. 98, No. 6, pp. 2795–2805, doi: 10.1785/0120070192, 2008.

Graziani, L., Maramai, A., and Tinti, S.: A revision of the 1783–1784 Calabrian (southern Italy) tsunamis, Nat. Hazards Earth Syst. Sci., 6, 1053–1060, 2006.

Guidoboni, E., Ferrari, G., Mariotti, D., Comastri, A., Tarabusi, G., and Valensise, G.: CFTI4Med, Catalogue of Strong Earthquakes in Italy (461 B.C.-1997) and Mediterranean Area (760 B.C.-1500). INGV-SGA. http://storing.ingv.it/cfti4med/, 2007.

Harbitz, C.B., Løvholt, F., and Bungum H.: Submarine landslide tsunamis: how extreme and how likely?, Nat Hazards (2014) 72:1341–1374, DOI 10.1007/s11069-013-0681-3, 2013.

Jarvis, A., Reuter, H.I., Nelson, A., Guevara, E.: Hole-filled seamless SRTM data V4, International Centre for Tropical Agriculture (CIAT), available from http://srtm.csi.cgiar.org, 2008.

Leonardi, M., Azzaro, F., Azzaro, M., Caruso, G., Mancuso, M., Monticelli, L.S., Maimone, G., La Ferla, R., Raffa, F., Zaccone, R.: A multidisciplinary study of the Cape Peloro brackish area (Messina, Italy): characterisation of trophic conditions, microbial abundances and activities. Marine Ecology 30 (Suppl. 1), 33–42. DOI: 10.1111/j.1439-0485.2009.00320.x, 2009.

Manganaro, A., Pulicanò, G., Sanfilippo, M.: Temporal evolution of the area of Capo Peloro (Sicily, Italy) from pristine site into urbanized area. TWB, Transit. Waters Bull. 5 (2011), n. 1, 23-31. DOI: 10.1285/i1825229Xv5n1p23, 2011.

Masson, D.G., Harbitz, C.B., Wynn, R.B., Pedersen, G. and Løvholt, F.: Submarine landslides: processes, triggers and hazard prediction, Phil. Trans. R. Soc. A 2006 364, 2009-2039, doi: 10.1098/rsta.2006.1810, 2006.

5 Mazzanti, P. and Bozzano, F.: Revisiting the February 6th 1783 Scilla (Calabria, Italy) landslide and tsunami by numerical simulation, Mar Geophys Res, 32:273–286, DOI 10.1007/s11001-011-9117-1, 2011.

Mercalli, G.: Alcuni risultati ottenuti dallo studio del terremoto calabrese dell'8 settembre 1905, Atti dell' Accademia Pontoniana di Napoli, 36, p.1-9 (in Italian), 1906.

10

Minasi, G.: Continuazione ed appendice sopra i tremuoti descritti nella relazione colla data di Scilla de 30 settembre 1783, con altro che accadde in progresso, Messina (in Italian), 1785.

Pantosti, D., Barbano, M. S., Smedile, A., De Martini, P. M., Tigano, G.: Geological evidence of paleotsunamis at Torre
15 degli Inglesi (northeast Sicily), Geophysical Research Letters, vol. 35, L05311, doi:10.1029/2007GL032935, 2008.

Papadopoulos, G. A., Gràcia, E., Urgeles, R., Sallares, V., De Martini, P.M., Pantosti, D., González, M., Yalciner, A.C., Mascle, J., Sakellariou, D., Salamon, A., Tinti, S., Karastathis, V., Fokaefs, A., Camerlenghi, A., Novikova, T., Papageorgiou, A.: Historical and pre-historical tsunamis in the Mediterranean and its connected seas: Geological signatures,
20 generation mechanisms and coastal impacts, Marine Geology 354 (2014) 81–109, doi: 10.1016/j.margeo.2014.04.014, 2014.

Porfido, S., Esposito, E., Violante, C., Molisso, F., Sacchi, M. and Spiga, E.: Earthquakes-Induced Environmental Effects in Coastal Area: Some Example in Calabria and Sicily (Southern Italy). Marine Research at CNR Dta. ISSN 2239-5172, 2011.

25 Randazzo, G., Cigala, C., Crupi, A., Lanza, S.: The natural causes of shoreline evolution of Capo Peloro, the northernmost point of Sicily (Italy). In: Green, A.N. and Cooper, J.A.G. (eds.), Proceedings 13th International Coastal Symposium (Durban, South Africa), Journal of Coastal Research, Special Issue No. 70, pp. 199-204, ISSN 0749-0208, 2014.

Sarconi, M.: Istoria de' fenomeni del tremuoto avvenuto nelle Calabrie e nel Valdemone nell'anno 1783, Napoli (in Italian),
30 1784.

Spallanzani, L.: Viaggi alle Due Sicilie e in alcune parti dell'Appennino, tomo IV, 145–155 (in Italian), 1795.

Tinti, S. and Guidoboni, E.: Revision of the tsunami occurred in 1783 in Calabria and Sicily (Italy), Science of Tsunami Hazards, 6, 17-22, 1988.

Tinti, S. and Piatanesi, A.: Finite-element simulations of the 5 February 1783 Calabrian tsunami, Phys. Chem. Earth, 21, 39-43, 1996.

Tinti, S. and Tonini, R.: The UBO-TSUFD tsunami inundation model: validation and application to a tsunami case study focused on the city of Catania, Italy, Nat. Hazards Earth Syst. Sci., 13, 1795–1816, www.nat-hazards-earth-syst-sci.net/13/1795/2013/, doi: 10.5194/nhess-13-1795-2013, 2013.

Tinti, S., Bortolucci, E., and Vannini, C.: A block-based theoretical model suited to gravitational sliding, Natural Hazards, 16, 1-28, 1997.

Tinti, S., Maramai, A., Graziani, L.: The Italian Tsunami Catalogue (ITC), Version 2. http://www.ingv.it/servizi-e-risorse/BD/catalogotsunami/catalogo-degli-tsunami-italiani, 2007.

Tinti, S., Chiocci, F.L., Zaniboni, F., Pagnoni, G., and de Alteriis, G.: Numerical simulation of the tsunami generated by a past catastrophic landslide on the volcanic island of Ischia, Italy, Mar Geophys Res (2011) 32:287–297, DOI: 10.1007/s11001-010-9109-6, 2011.

Torcia, M.: Tremuoto avvenuto nella Calabria e a Messina all 5 febbrajo 1783 descritto da Michele Torcia- Archiviario di S. M. Siciliana e Membro della Accademia Regia, Napoli, 1783.

Vela, J., Pérez, B., González, M., Otero, L., Olabarrieta, M., Canals, M., and Casamor, J.L.: Tsunami resonance in the Palma de Majorca bay and harbour induced by the 2003 Boumerdes-Zemmouri Algerian earthquake (Western Mediterranean), in: Proceedings of 32nd International Conference on Coastal Engineering (ICCE 2010), ASCE, 2010.

Vivenzio, G.: Historia dei tremuoti avvenuti nella provincia di Calabria ulteriore e nella città di Messina nell'anno 1783, Napoli (in Italian), 1788.

Wang, L., Zaniboni, F., Tinti, S., Zhang, X.: Reconstruction of the 1783 Scilla landslide, Italy: numerical investigations on the flow-like behavior of landslides. Landslides. DOI 10.1007/s10346-019-01151-5, 2019.

Zaniboni, F. and Tinti, S.: Numerical simulations of the 1963 Vajont landslide, Italy: application of 1D Lagrangian modelling, Natural Hazards, 70:567–592, doi: 10.1007/s11069-013-0828-2, 2014.

Zaniboni, F., Pagnoni, G., Tinti, S., Della Seta, M., Fredi, P., Marotta, E., and Orsi, G.: The potential failure of Monte Nuovo at Ischia Island (Southern Italy): numerical assessment of a likely induced tsunami and its effects on a densely inhabited area, Bulletin of Volcanology 75:763, doi: 10.1007/s00445-013-0763-9, 2013.

5 Zaniboni, F., Armigliato, A., Pagnoni, G., and Tinti, S.: Continental margins as a source of tsunami hazard: the 1977 Gioia Tauro (Italy) landslide-tsunami investigated through numerical modelling, Marine Geology 357 (2014) 210-217, doi: 10.1016/j.margeo.2014.08.011, 2014a.

Zaniboni, F., Pagnoni, G., Armigliato, A., Elsen, K., and Tinti, S.: Investigations on the possible source of the 2002 landslide
10 tsunami in Rhodes, Greece, through numerical techniques. G. Lollino, A. Manconi, J. Locat, Y. Huang, M. Canals Ardilas (eds.), Engineering Geology for Society and Territory – Volume 4, DOI: 10.1007/978-3-319-08660-6_17, © Springer International Publishing Switzerland, 2014b.

Zaniboni, F., Pagnoni, G., Armigliato, A., Tinti, S., Iglesias, O., and Canals, M.: Numerical simulation of the BIG'95 debris
15 flow and of the generated tsunami. G. Lollino, A. Manconi, J. Locat, Y. Huang, M. Canals Ardilas (eds.), Engineering Geology for Society and Territory – Volume 4, DOI: 10.1007/978-3-319-08660-6_19, © Springer International Publishing Switzerland, 2014c.

Zaniboni, F., Armigliato, A., and Tinti, S.: A numerical investigation of the 1783 landslide-induced catastrophic tsunami in
20 Scilla, Italy, Nat Hazards, 84: S455–S470. DOI 10.1007/s11069-016-2461-3, 2016.

Figure 1: The logo of Copernicus Publications.